Recognition of different base tetrads by RHAU (DHX36): X-ray crystal structure of the G4 recognition motif bound to the 3'-end tetrad of a DNA G-quadruplex

Brahim Heddi, Vee Vee Cheong, Emmanuelle Schmitt, Yves Mechulam, Anh Tuân Phan

Recognition of different base tetrads by RHAU: X-ray crystal structure of the G4 recognition motif bound to the 3'-end tetrad of a DNA G-quadruplex

Brahim Heddi[1,2*], Vee Vee Cheong[1], Emmanuelle Schmitt[3],
Yves Mechulam[3] and Anh Tuân Phan[1*]

[1]School of Physical and Mathematical Sciences, Nanyang Technological University, 21 Nanyang Link, Singapore 637371, Singapore

[2]Laboratoire de Biologie et de Pharmacologie Appliquée, CNRS UMR 8113, Ecole Normale Supérieure Paris-Saclay, 61 Avenue du président Wilson, Cachan 94235, France

[3]Laboratoire de Biochimie, UMR 7654, Ecole Polytechnique, Centre National de la Recherche Scientifique, Palaiseau 91128, France

*Corresponding author: phantuan@ntu.edu.sg and brahim.heddi@ens-cachan.fr

Running title: Protein recognition of different base tetrads

ABSTRACT

G-quadruplexes (G4) are secondary structures of nucleic acids that can form in cells and have diverse biological functions. Several biologically important proteins interact with G-quadruplexes, of which RHAU – a helicase from the DEAH-box superfamily, was shown to bind and unwind G-quadruplexes efficiently. We report a high-resolution (1.5 Å) X-ray co-crystal structure of an N-terminal fragment of RHAU bound to the exposed tetrad of a parallel-stranded G-quadruplex. The RHAU peptide folds into an L-shaped α–helix, and binds to the G-quadruplex through π–stacking and electrostatic interactions. X-ray crystal structure of our complex identified key amino-acid residues important for G-quadruplex-peptide binding interaction at the 3'-end G•G•G•G tetrad. Together with previous solution and crystal structures of RHAU bound to the 5'-end G•G•G•G and A•T•G•G tetrads, our crystal structure highlights the occurrence of a robust G-quadruplex recognition motif within RHAU that can adapt to different accessible tetrads.

Keywords: G-quadruplex; X-ray crystallography; RHAU helicase; DHX36; G4R1; DEAH-box family.

INTRODUCTION

G-quadruplexes are four-stranded nucleic acid secondary structures formed by the stacking of G-tetrads (planar G•G•G•G structure formed by Hoogsteen base pairing) and stabilized by cations [1]. G-quadruplexes are polymorphic and can adopt diverse topologies [2, 3] as exemplified by parallel (all four strands in the same direction) and non-parallel (one or two strands in the opposite direction) G-quadruplexes.

G-quadruplexes form in cells[4-6], and are involved in key cellular processes including transcription, replication and translation, and implicated in genomic instability and aging[7-12]. Several biologically relevant proteins interact with G-quadruplexes[6, 13] by promoting G-quadruplex formation/stabilization, or through the deformation of G-quadruplexes[12]. Among them several biologically important helicases bind and unwind G-quadruplexes with high affinity and efficiency[14]. However, molecular details on how proteins interact with G-quadruplex remain very scarce [15].

RHAU (also called DHX36), a helicase of the DEAH-box superfamily which binds and unwinds RNA and DNA G-quadruplexes with high affinity and efficiency[16-19], is reported to exhibit a 100-fold binding preference for parallel G-quadruplexes as compared to non-parallel G-quadruplexes[20]. RHAU is composed of an N-terminal domain containing the RHAU-specific motif (RSM), a helicase core and a C-terminal domain, and is conserved across numerous organisms[17]. RHAU is involved in spermatogenesis[21-23], heart development during embryogenesis[24], hematopoiesis[25], and is shown to regulate several RNA[26, 27] and mRNA[24, 28, 29], likely through interaction with important G-quadruplex forming sequences present in the 5'- or 3'-UTR.

In 2015, we reported a high-resolution NMR solution structure of the N-terminal RSM-containing 18-aa fragment of RHAU (***Rhau18***) in complex with a parallel-stranded G-quadruplex[20]. The solution structure identified ***Rhau18*** to form an α-helix G-quadruplex recognition motif, with the peptide bound to the 5'-end terminal parallel G-quadruplex via hydrophobic/stacking and electrostatic interactions. As this peptide-quadruplex binding mode resembles the binding mode of most G-quadruplex ligands[30], our NMR solution structure suggested the preference of RHAU for parallel-stranded G-quadruplex to be mainly due to their G-tetrad accessibility and steric hindrance of the protein[20].

The recognition mode of RHAU for G-quadruplex identified in ***Rhau18*** was similarly observed in a recent X-ray crystal structure of a truncated bovine RHAU co-crystallized with a parallel G-quadruplex[31]. The structure identified a bovine RHAU α-helix fragment to utilize hydrophobic/stacking and electrostatic interactions to bind to a 5'-end A•T•G•G tetrad (Figure S1A). Structural comparison between the bovine RHAU-quadruplex complex and human RHAU-quadruplex complex finds key residues participating in the binding interaction between peptide and DNA to be highly conserved across the two species, with very similar N-terminal amino acids identified to interact with an accessible 5'-end tetrad (Figure S1B). This finding reinforced our hypothesis of RHAU preferentiality to parallel G-quadruplex to be dependent on the availability of accessible tetrads[20]. Binding affinity between the full-length RHAU and a G-quadruplex can be further enhanced by electrostatic interactions between the negatively-charged backbone of the G-quadruplex and the positively-charged cavity of RHAU[31, 32].

Rhau18 was also shown to bind to a 3'-end G-tetrad when the 5'-end tetrad binding interface is occupied by another ***Rhau18*** peptide [20]. It was recently shown that RHAU was pulling one residue at a time with 3' to 5' directionality to destabilize and resolve the G-quadruplex structure[31]. With the 3'-end G-tetrad possessing opposite polarity to a 5'-end tetrad, the binding of RHAU to a 3'-end G-tetrad may imply a different unfolding mechanism to be involved. Through structural comparison of RHAU-quadruplex complexes with different peptide-quadruplex binding interface, better understanding of how RHAU adapts to different tetrad polarity could be achieved, and possibly provide clues on its unwinding mechanism.

In this study, we report the co-crystallization of a dimeric parallel-stranded DNA G-quadruplex with exposed 3'-end G-tetrad in complex with a 29-amino acid peptide extracted from the N-terminal human helicase RHAU. Our X-ray crystal structure shows the DNA to assemble as a dimeric parallel-stranded G-quadruplex, with the peptide interacting at the 3'-end terminal G-tetrad. The peptide conformation in the co-crystal structure highly resembles the N-terminal domain of RHAU in earlier reported structures[20, 31], adopting a predominantly α–helical structure. Analysis of the X-ray co-crystal structure finds the peptide to interact with the G-quadruplex through extensive CH/π– CH_3/π–stacking and electrostatic interactions using conserved positively charged residues. Our structure suggests the N-terminal binding domain of RHAU to possess a robust motif capable of binding different G-tetrad polarity.

RESULTS AND DISCUSSION

Structure determination of *Rhau29-T95* co-crystal complex

Crystallization trials were conducted on a 29-aa RSM-containing N-terminal RHAU fragment named ***Rhau29*** (N_{term}-HPGHLKGREIGMWYAKKQGQKNKEAERQE-C_{term}) and the G-

quadruplex forming sequence $d(GGGT)_4$ named ***T95***. The ***Rhau29-T95*** complex was successfully crystallized (see Methods), with crystals of $P2_1$ space group diffracted X-rays to 1.5 Å resolution. The structure was solved using molecular replacement with a parallel-stranded G-quadruplex (coordinates from the PDB code 2LK7 without terminal thymine residues) [33] as a starting model and refined using REFMAC [34] to 1.5 Å resolution (Table 1 and Figure 1).

Figure 1A illustrates a representative portion of the final electron density of the ***Rhau29-T95*** complex, showing two ***Rhau29*** peptides bound to a dimeric ***T95*** G-quadruplex on the exposed 3'-end tetrads. The asymmetric unit of the X-ray crystal structure is composed of two ***Rhau29-T95*** complexes (Figure S2) which are nearly identical (all-atom RMSD = 0.78 Å, excluding the terminal thymine residues, Figure S3A). Analysis of the asymmetrical unit finds the four individual peptide-quadruplex subunits (each consisting of one DNA molecule and one ***Rhau29*** molecule) to be very similar (pairwise RMSD = 0.74±0.1 Å, Figure S3B), with notable structural differences found only in the terminal thymine residues as well as side chain of lysine residues. Five K^+ ions are found between the G-tetrads, within the subunits and at the stacking interface between the two subunits (Figure 1A). A total of 262 water molecules are distributed along the medium grooves and around the phosphate groups. In our electron density map, 48 amino acids corresponding to the 12 C-terminal residues in each of the four ***Rhau29*** molecules in the asymmetric unit could not be seen. The final refinement of the complex led to an R_{free} equal to 0.2448 (R_{work} = 0.1853), in which a long mobile segment within the four ***Rhau29*** molecules likely contributed to the relatively high R_{free} value.

Two *Rhau29* peptides encase a dimeric G-quadruplex

In the ***Rhau29-T95*** complex, the dimeric G-quadruplex in our X-ray crystal structure consists of two stacked parallel-stranded G-quadruplex subunits. Within each G-quadruplex subunit, the G-tetrads adopt the same hydrogen-bond directionality (G1•G5•G9•G13, G2•G6•G10•G14 and G3•G7•G11•G15), and the two subunits are stacked via their 5'-5'-end interface (Figure 1B) with partial overlap between the 5/6-membered ring of the guanine bases of each subunit (*i.e.* G1/G9*, G5/G5*, G9/G1*, G13/G13* – asterisks denote the second subunit). Such stacking mode has been observed in NMR-derived structures of similar G-quadruplex-forming sequences which also adopts a dimeric parallel-stranded G-quadruplex conformation (Figure S4)[35]. The DNA is encased between the two peptide molecules (Figure 1). Our structure shows the two ***Rhau29*** molecules to bind onto the 3'-end interfaces of the dimeric G-quadruplex, with each peptide covering the exposed G-tetrad of the dimeric G-quadruplex. Analysis of free dimeric parallel-stranded G-quadruplex solution structure and the ***Rhau29-T95*** complex X-ray crystal structure finds the 5'-5' stacking interface between the G-quadruplex subunits to remain unperturbed by the binding of ***Rhau29*** (Figure S4).

***Rhau29* peptides folds into an L-shaped α-helix**

The peptide presents an L-shaped structure with an α-helix spanning residues 7 to 15, with Leu5, Ile10, Trp13 and Tyr14 forming the hydrophobic core (Figure 2, Figure S5). The missing 12 residues at C-terminal of each ***Rhau29*** molecule could indicate that these residues are structured only in the presence of the full-length protein when bound to a G-quadruplex, with mutagenesis data of bovine RHAU suggesting a partial ligand-induced protein folding for the N-terminal RHAU fragment[31].

Previously, we have solved the solution structure of an 18-aa peptide ***Rhau18*** (N_{term}-SMHPGHLKGREIGMWYAKKQ-C_{term}) bound to the 5'-end G-tetrad of a parallel-stranded G-quadruplex[20], and recently the X-ray crystal structure of the bovine RHAU containing the RHAU-specific motif ***RhauB*** (N_{term}-PGHLKGREIGLWYAKKQ-C_{term}) bound to a 5'-end A•T•G•G tetrad of a parallel G-quadruplex intermediate was reported[31]. The ***Rhau18*** contains an α-helical L-shaped motif found to be critical for G-quadruplex binding, which is preserved in the C-terminal extended peptide ***Rhau29*** and similarly retained in bovine ***RhauB***. Structure comparison of ***Rhau29, RhauB*** and ***Rhau18*** shows the three peptide cores to be highly similar (pairwise r.m.s.d. = 0.8±0.1 Å using backbone atoms from residue 3 to 16) (Figure S5). However, the orientation of the N- and C-terminal residues in ***Rhau18, RhauB*** and ***Rhau29*** structures differs. This difference could be explained by the presence of several interactions in the crystal packing: interactions between His3, Pro4, Gly5, His6 and W15 of ***Rhau29*** and the sugar-phosphate backbone of G9, G10, and G11 and T8 (Figure S6), with similar interactions being observed in the X-ray crystal structure of the bovine RHAU[31]. The N-terminal region of each peptide differs minutely between the structures, with ***Rhau18*** containing two extra residues (Ser and Met) from the plasmid vector[20]. Additionally, the C-terminal tail of ***Rhau29*** in the X-ray crystal structure is facing the 3'-end and 5'-end terminal DNA residues, while the C-terminal tail of ***Rhau18*** in the NMR structure is facing the middle thymine loop.

Binding of *Rhau29* to a different tetrad polarity

In our structure, an optimal fit is found between the peptide and the 3'-end G-tetrad. The ***Rhau29*** peptide face interacting with the G-quadruplex is remarkably planar, with Cα of Gly11 pointing toward the center of the G-tetrad (Figure S7). Electrostatic interactions are found between three

conserved residues of ***Rhau29*** (Lys6, Arg8 and Lys17)[23] and the phosphate groups of ***T95***. Within the asymmetric unit, the position of these residues differs slightly between the different peptide-DNA complexes (Figure S8). This is reflected by higher temperature factors for these peptide side chains (43.82 ± 11.96, as compared to the mean temperature factors for all peptide side chains, 27.00 ± 11.96). Extensive CH-π and CH_3-π interaction are also found between His1, Gly7, Arg8, Ile10, Gly11, Met12 and Tyr14 with the guanine bases (Figure 2B, 2D).

Our ***Rhau29-T95*** structure shows ***Rhau29*** to bind to the 3'-end G-tetrad, in contrast to structures of similar RHAU fragments (***Rhau18*** and ***RhauB***) bound to the 5'-end tetrad[20, 31]. Structurally, the 5'- and 3'-end G-tetrads in a parallel-stranded G-quadruplex are quite different: (i) the exposed face polarity is reversed (Figure 3), which was shown to influence the stacking energy[36]; (ii) the sugar and phosphate group orientations in a 3'-end interface are different from those in a 5'-end interface (Figure 3). These differences can influence the recognition mode and/or the binding affinity of G-quadruplex-interacting molecules, as recently demonstrated for the binding of small-molecule ligands to different G-tetrad surfaces[37].

RHAU contains a versatile G-quadruplex binding motif

The ***Rhau29-T95*** co-crystal structure provides the first high-resolution data for the binding of a fragment of RHAU onto the 3'-end G-tetrad of a G-quadruplex. The X-ray crystal structure agrees with the reported NMR data of RHAU, where the 5'-end and 3'-end G-tetrads have been identified as G-quadruplex binding sites[20]. The N-terminal 18-aa RHAU motif appears to act as an independent domain capable of docking onto a G-quadruplex with accessible G-tetrads, in which our data demonstrated the recognition of G-quadruplex by RHAU to be malleable and adaptive in the binding of 5'- or 3'-end accessible tetrads despite differences in tetrad polarity (5'-

vs. 3'-end)[20] or composition (G•G•G•G vs. A•T•G•G)[20, 31]. Within the RHAU G-quadruplex recognition motif, the conserved residues Arg8 and Ile10 were found to play a critical role in resolving G-quadruplexes by the helicase[38].

Dimeric G-quadruplexes were shown to be potentially formed in TERRA[39, 40], human telomerase RNA[41], as well as the human CEB1 minisatellites[42, 43]. In the context of a dimeric G-quadruplex, it is speculated that the protein may be positioned on each available side of the G-quadruplex dimer to facilitate the unwinding of each individual G-quadruplex subunit. It is anticipated that RHAU helicase will use the same binding principles, as evidenced here, in the recognition of different tetrads such as G•C•G•C tetrads[2, 44], or even in triads[45].

MATERIALS AND METHODS

Sample preparation

DNA oligonucleotides were chemically synthesized on an ABI 394 DNA/RNA synthesizer using standard oligonucleotide synthesis cycle. Oligonucleotides were cleaved from the solid support and deprotected with ammonium hydroxide, purified using Poly-Pak cartridges (Glen Research) and dialyzed successively against water, KCl solution and water prior to lyophilization. Peptides used in X-ray crystallization study were purchased from Chempeptide Ltd. DNA and peptide samples were reconstituted in potassium cacodylate buffer.

Crystallization, X-ray crystallography and structure refinement

Crystallization assays were performed with sitting-drop method, using a solution of ***T95*** (2 mM) and ***Rhau29*** (1.5 mM) in buffer containing 100 mM potassium cacodylate buffer (pH 6.5), 100

mM potassium chloride. Initial screening was done with Natrix commercial screens (Hampton Research). Monoclinic crystals (space group $P2_1$) were obtained using 55% methylpentanediol as precipitating agent, in the presence of 40 mM sodium cacodylate (pH 6.0), 80 mM potassium chloride and 12 mM spermine tetrahydrochloride. For data collection, crystals were directly flash frozen in liquid nitrogen. Data were collected from a single crystal at the Swiss Light Source beamline (λ= 1.00 Å; Zurich, Switzerland) equipped with a Pilatus detector, and processed using XDS [46]. Data collection statistics are summarized in Table 1. The structure was solved by molecular replacement, using PHASER[47] and refined to 1.5 Å resolution. The coordinates of the DNA residues, except the terminal thymines, from the NMR structure of a parallel-stranded G-quadruplex [33] were used as a search model. The model was refined and completed with ions and water molecules, following several cycles of manual building using Coot[48] and energy minimization using REFMAC [34]. The final model contains all 16 DNA nucleotides, 17 out of 29 peptide residues, 5 potassium ions, and 262 water molecules. Structures were further visualized using PYMOL viewer program, that was also used to generate the figures[49].

Data deposition

The coordinates for the crystal structure of the ***Rhau29-T95*** complex have been deposited in the Protein Data Bank (PDB ID: **6Q6R**)

FUNDING

This work was supported by Singapore Ministry of Education Academic Research Fund Tier 2 (MOE2018-T2-2-029). No competing financial interests have been declared.

ACKNOWLEDGEMENTS

We thank Julien Lescar and Abbas El Sahili for collecting the diffraction data.

REFERENCES

[1] Davis JT. G-quartets 40 years later: from 5'-GMP to molecular biology and supramolecular chemistry. Angew. Chem. Int. Ed. Engl. (2004) 43:668-98.

[2] Patel DJ, Phan AT, Kuryavyi V. Human telomere, oncogenic promoter and 5′-UTR G-quadruplexes: diverse higher order DNA and RNA targets for cancer therapeutics. Nucleic Acids Res. (2007) 35:7429-55.

[3] Phan AT. Human telomeric G-quadruplex: structures of DNA and RNA sequences. FEBS J. (2010) 277:1107-17.

[4] Biffi G, Tannahill D, McCafferty J, Balasubramanian S. Quantitative visualization of DNA G-quadruplex structures in human cells. Nat. Chem. (2013) 5:182-6.

[5] Henderson A, Wu Y, Huang YC, Chavez EA, Platt J, Johnson FB, et al. Detection of G-quadruplex DNA in mammalian cells. Nucleic Acids Res. (2014) 42:860-9.

[6] Lipps HJ, Rhodes D. G-quadruplex structures: in vivo evidence and function. Trends Cell Biol. (2009) 19:414-22.

[7] Cahoon LA, Seifert HS. An alternative DNA structure is necessary for pilin antigenic variation in Neisseria gonorrhoeae. Science. (2009) 325:764-7.

[8] Kumari S, Bugaut A, Huppert JL, Balasubramanian S. An RNA G-quadruplex in the 5' UTR of the NRAS proto-oncogene modulates translation. Nat. Chem. Biol. (2007) 3:218-21.

[9] Lopes J, Piazza A, Bermejo R, Kriegsman B, Colosio A, Teulade-Fichou MP, et al. G-quadruplex-induced instability during leading-strand replication. EMBO J. (2011) 30:4033-46.

[10] Maizels N, Gray LT. The G4 genome. PLoS Genet. (2013) 9:e1003468.

[11] Murat P, Balasubramanian S. Existence and consequences of G-quadruplex structures in DNA. Curr. Opin. Genet. Dev. (2014) 25:22-9.

[12] Rhodes D, Lipps HJ. G-quadruplexes and their regulatory roles in biology. Nucleic Acids Res. (2015) 43:8627-37.

[13] Oganesian L, Bryan TM. Physiological relevance of telomeric G-quadruplex formation: a potential drug target. Bioessays. (2007) 29:155-65.

[14] Sauer M, Paeschke K. G-quadruplex unwinding helicases and their function in vivo. Biochem. Soc. Trans. (2017) 45:1173-82.

[15] Mendoza O, Bourdoncle A, Boule JB, Brosh RM, Jr., Mergny JL. G-quadruplexes and helicases. Nucleic Acids Res. (2016) 44:1989-2006.

[16] Creacy SD, Routh ED, Iwamoto F, Nagamine Y, Akman SA, Vaughn JP. G4 resolvase 1 binds both DNA and RNA tetramolecular quadruplex with high affinity and is the major source of tetramolecular quadruplex G4-DNA and G4-RNA resolving activity in HeLa cell lysates. J. Biol. Chem. (2008) 283:34626-34.

[17] Lattmann S, Giri B, Vaughn JP, Akman SA, Nagamine Y. Role of the amino terminal RHAU-specific motif in the recognition and resolution of guanine quadruplex-RNA by the DEAH-box RNA helicase RHAU. Nucleic Acids Res. (2010) 38:6219-33.

[18] Meier M, Patel TR, Booy EP, Marushchak O, Okun N, Deo S, et al. Binding of G-quadruplexes to the N-terminal recognition domain of the RNA helicase associated with AU-rich element (RHAU). J. Biol. Chem. (2013) 288:35014-27.
[19] Vaughn JP, Creacy SD, Routh ED, Joyner-Butt C, Jenkins GS, Pauli S, et al. The DEXH protein product of the DHX36 gene is the major source of tetramolecular quadruplex G4-DNA resolving activity in HeLa cell lysates. J. Biol. Chem. (2005) 280:38117-20.
[20] Heddi B, Cheong VV, Martadinata H, Phan AT. Insights into G-quadruplex specific recognition by the DEAH-box helicase RHAU: Solution structure of a peptide-quadruplex complex. Proc. Natl. Acad. Sci. U.S.A. (2015) 112:9608-13.
[21] Fu JJ, Li LY, Lu GX. Molecular cloning and characterization of human DDX36 and mouse Ddx36 genes, new members of the DEAD/H box superfamily. Acta Biochim. Biophys. Sin. (Shanghai). (2002) 34:655-61.
[22] Gao X, Ma W, Nie J, Zhang C, Zhang J, Yao G, et al. A G-quadruplex DNA structure resolvase, RHAU, is essential for spermatogonia differentiation. Cell Death Dis. (2015) 6:e1610.
[23] Lattmann S, Giri B, Vaughn JP, Akman SA, Nagamine Y. Role of the amino terminal RHAU-specific motif in the recognition and resolution of guanine quadruplex-RNA by the DEAH-box RNA helicase RHAU. Nucleic Acids Res. (2010) 38:6219-33.
[24] Nie J, Jiang M, Zhang X, Tang H, Jin H, Huang X, et al. Post-transcriptional Regulation of Nkx2-5 by RHAU in Heart Development. Cell Rep. (2015) 13:723-32.
[25] Lai JC, Ponti S, Pan D, Kohler H, Skoda RC, Matthias P, et al. The DEAH-box helicase RHAU is an essential gene and critical for mouse hematopoiesis. Blood. (2012) 119:4291-300.
[26] Lattmann S, Stadler MB, Vaughn JP, Akman SA, Nagamine Y. The DEAH-box RNA helicase RHAU binds an intramolecular RNA G-quadruplex in TERC and associates with telomerase holoenzyme. Nucleic Acids Res. (2011) 39:9390-404.
[27] Booy EP, Meier M, Okun N, Novakowski SK, Xiong S, Stetefeld J, et al. The RNA helicase RHAU (DHX36) unwinds a G4-quadruplex in human telomerase RNA and promotes the formation of the P1 helix template boundary. Nucleic Acids Res. (2012) 40:4110-24.
[28] Booy EP, Howard R, Marushchak O, Ariyo EO, Meier M, Novakowski SK, et al. The RNA helicase RHAU (DHX36) suppresses expression of the transcription factor PITX1. Nucleic Acids Res. (2014) 42:3346-61.
[29] Huang H, Suslov NB, Li NS, Shelke SA, Evans ME, Koldobskaya Y, et al. A G-quadruplex-containing RNA activates fluorescence in a GFP-like fluorophore. Nat. Chem. Biol. (2014) 10:686-U128.
[30] Ohnmacht SA, Neidle S. Small-molecule quadruplex-targeted drug discovery. Bioorg. Med. Chem. Lett. (2014) 24:2602-12.
[31] Chen MC, Tippana R, Demeshkina NA, Murat P, Balasubramanian S, Myong S, et al. Structural basis of G-quadruplex unfolding by the DEAH/RHA helicase DHX36. Nature. (2018) 558:465-9.

[32] Chen WF, Rety S, Guo HL, Dai YX, Wu WQ, Liu NN, et al. Molecular Mechanistic Insights into Drosophila DHX36-Mediated G-Quadruplex Unfolding: A Structure-Based Model. Structure. (2018) 26:403-15.
[33] Do NQ, Phan AT. Monomer-dimer equilibrium for the 5'-5' stacking of propeller-type parallel-stranded G-quadruplexes: NMR structural study. Chemistry. (2012) 18:14752-9.
[34] Murshudov GN, Skubak P, Lebedev AA, Pannu NS, Steiner RA, Nicholls RA, et al. REFMAC5 for the refinement of macromolecular crystal structures. Acta Crystallogr. D. Biol. Crystallogr. (2011) 67:355-67.
[35] Do NQ, Lim KW, Teo MH, Heddi B, Phan AT. Stacking of G-quadruplexes: NMR structure of a G-rich oligonucleotide with potential anti-HIV and anticancer activity. Nucleic Acids Res. (2011) 39:9448-57.
[36] Lech CJ, Heddi B, Phan AT. Guanine base stacking in G-quadruplex nucleic acids. Nucleic Acids Res. (2013) 41:2034-46.
[37] Le DD, Di Antonio M, Chan LK, Balasubramanian S. G-quadruplex ligands exhibit differential G-tetrad selectivity. Chem Commun (Camb). (2015) 51:8048-50.
[38] Tippana R, Chen MC, Demeshkina NA, Ferre-D'Amare AR, Myong S. RNA G-quadruplex is resolved by repetitive and ATP-dependent mechanism of DHX36. Nat Commun. (2019) 10:1855.
[39] Martadinata H, Phan AT. Structure of human telomeric RNA (TERRA): stacking of two G-quadruplex blocks in K(+) solution. Biochemistry. (2013) 52:2176-83.
[40] Martadinata H, Heddi B, Lim KW, Phan AT. Structure of long human telomeric RNA (TERRA): G-quadruplexes formed by four and eight UUAGGG repeats are stable building blocks. Biochemistry. (2011) 50:6455-61.
[41] Martadinata H, Phan AT. Formation of a stacked dimeric G-quadruplex containing bulges by the 5'-terminal region of human telomerase RNA (hTERC). Biochemistry. (2014) 53:1595-600.
[42] Piazza A, Cui X, Adrian M, Samazan F, Heddi B, Phan AT, et al. Non-Canonical G-quadruplexes cause the hCEB1 minisatellite instability in Saccharomyces cerevisiae. Elife. (2017) 6.
[43] Adrian M, Ang DJ, Lech CJ, Heddi B, Nicolas A, Phan AT. Structure and conformational dynamics of a stacked dimeric G-quadruplex formed by the human CEB1 minisatellite. J. Am. Chem. Soc. (2014) 136:6297-305.
[44] Zhang N, Gorin A, Majumdar A, Kettani A, Chernichenko N, Skripkin E, et al. Dimeric DNA quadruplex containing major groove-aligned A-T-A-T and G-C-G-C tetrads stabilized by inter-subunit Watson-Crick A-T and G-C pairs. J. Mol. Biol. (2001) 312:1073-88.
[45] Heddi B, Martin-Pintado N, Serimbetov Z, Kari TM, Phan AT. G-quadruplexes with (4n - 1) guanines in the G-tetrad core: formation of a G-triad.water complex and implication for small-molecule binding. Nucleic Acids Res. (2016) 44:910-6.
[46] Kabsch W. Xds. Acta Crystallogr. D. Biol. Crystallogr. (2010) 66:125-32.

[47] McCoy AJ, Grosse-Kunstleve RW, Adams PD, Winn MD, Storoni LC, Read RJ. Phaser crystallographic software. J. Appl. Crystallogr. (2007) 40:658-74.
[48] Emsley P, Lohkamp B, Scott WG, Cowtan K. Features and development of Coot. Acta Crystallogr. D. Biol. Crystallogr. (2010) 66:486-501.
[49] Schrodinger, LLC. The PyMOL Molecular Graphics System, Version 1.3r1. 2010.

FIGURE LEGENDS

Figure 1. Crystal structure of ***Rhau29*** peptide and ***T95*** G-quadruplex. (**a**) Model of a dimer and the corresponding electron density (2mFc0-dFc map contoured at 1.0 σ). (**b**) Schematic view of the topology of the ***T95*** G-quadruplex dimer (**c**) ribbon view of four individual peptides/DNA complexes found in the asymmetric unit viewed from the front and (**d**) the top. Proteins are in green, DNA are in gray (backbone), cyan (Guanine bases), and orange (Thymine bases).

Figure 2. Molecular details of the DNA/peptide interaction. (**a**) and (**c**) Top and front ribbon views of one complex monomer. (**b**) and (**d**) Top- and front-views of the amino-acid residues interacting with the G-tetrads (only residues in direct contact with the tetrad are shown).

Figure 3. Comparison between X-ray (left) and NMR (right) structure. (**a**) Top view of a G-tetrad oriented in 3'- and 5'-end interfaces and (**b**) front view of peptide/DNA complex. Sugars are represented in ball and sticks view; O4' atoms are in red; Guanine residues are in cyan.

Table

Table 1. Data collection and refinement statistics

Data collection*	
Space group	$P2_1$
Cell dimensions	
a, b, c (Å)	56.27, 42.09, 61.11
α, β, γ (°)	90.0, 99.3, 90.0
Resolution (Å)	60.60 1.50
Rsym	0.083 (0.941)
I / σI	8.50 (1.34)
Completeness (%)	99.35 (96.25)
Redundancy	9.1 (5.6)
Refinement	
Resolution (Å)	44.75 - 1.50
Number of reflections	45457
Rwork / Rfree	0.1853/0.2448
Number of atoms	
DNA	1364
Protein	564
K^+	10
Water	265
B-factors ($Å^2$)	DNA 23.7 Protein 28.4 K^+ 11.1 Water 38.4
r.m.s.d.	
Bond lengths (Å)	0.019
Bond angles (°)	1.947

*A single crystal was used for data collection. Values in parentheses are for the highest-resolution shell.

Figure1

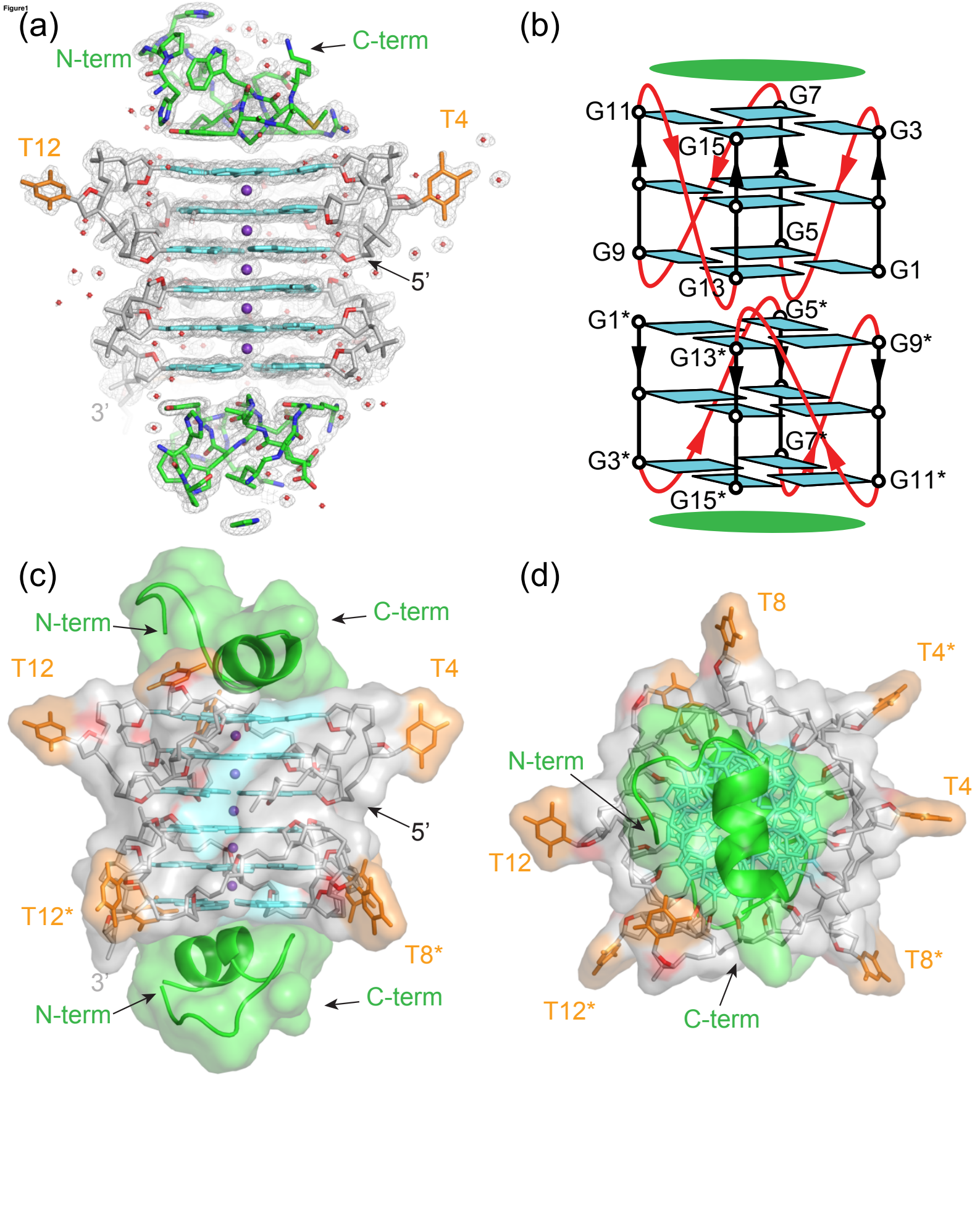
(a)
N-term
C-term
T4
T12
5’
3’
(b)
G11
G7
G3
G15
G5
G9
G1
G13
G1*
G5*
G9*
G13*
G7*
G3*
G11*
G15*
(c)
N-term
C-term
T12
T4
5’
T12*
T8*
3’
N-term
C-term
(d)
T8
T4*
N-term
T4
T12
T8*
T12*
C-term

Figure2

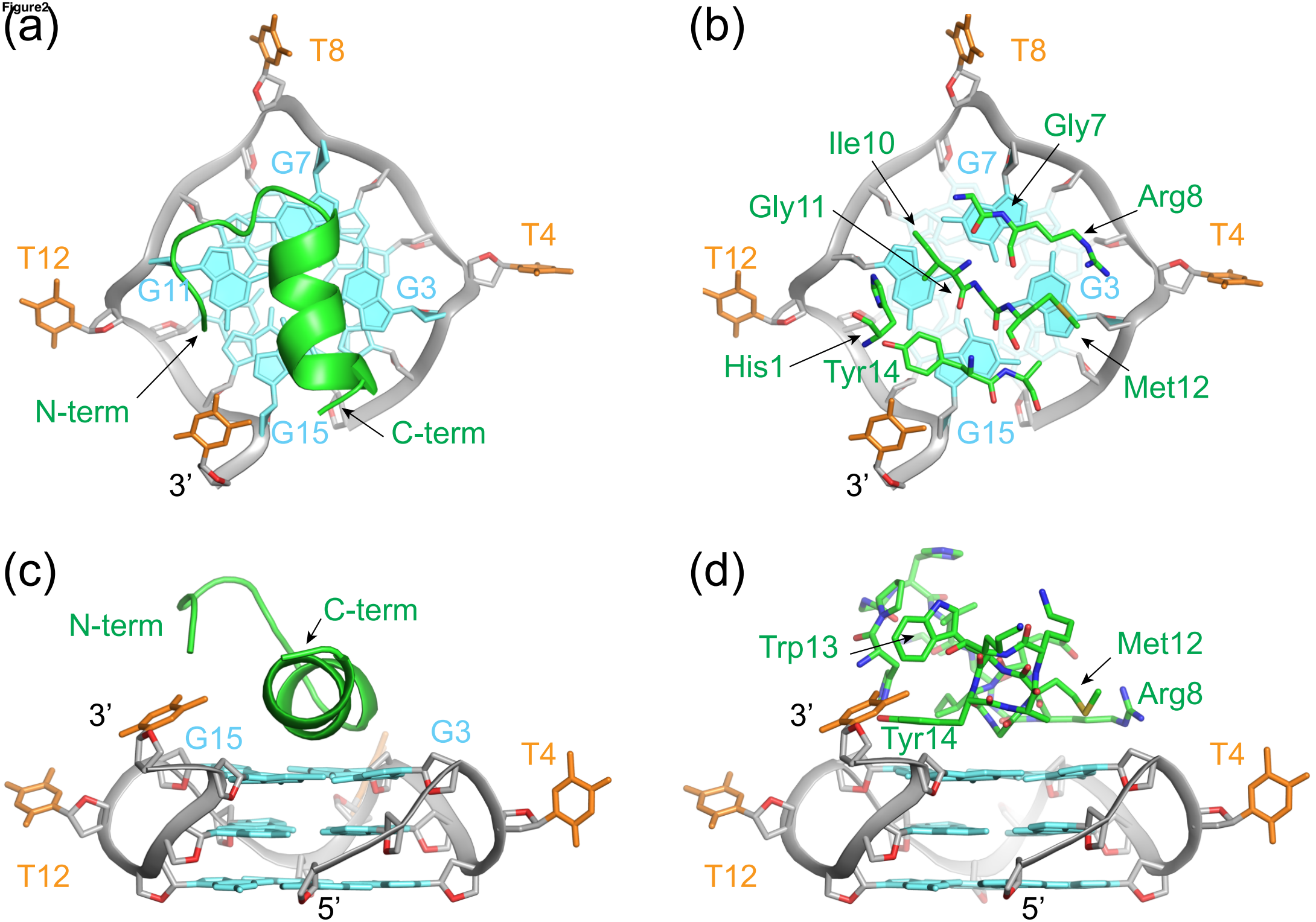
(a)
T8
G7
T4
T12
G11
G3
N-term
G15
C-term
3’
(b)
T8
Ile10
Gly7
G7
Gly11
Arg8
T4
T12
G3
His1
Tyr14
Met12
G15
3’
(c)
N-term
C-term
3’
G15
G3
T4
T12
5’
(d)
Trp13
Met12
Arg8
3’
Tyr14
T4
T12
5’

Figure2

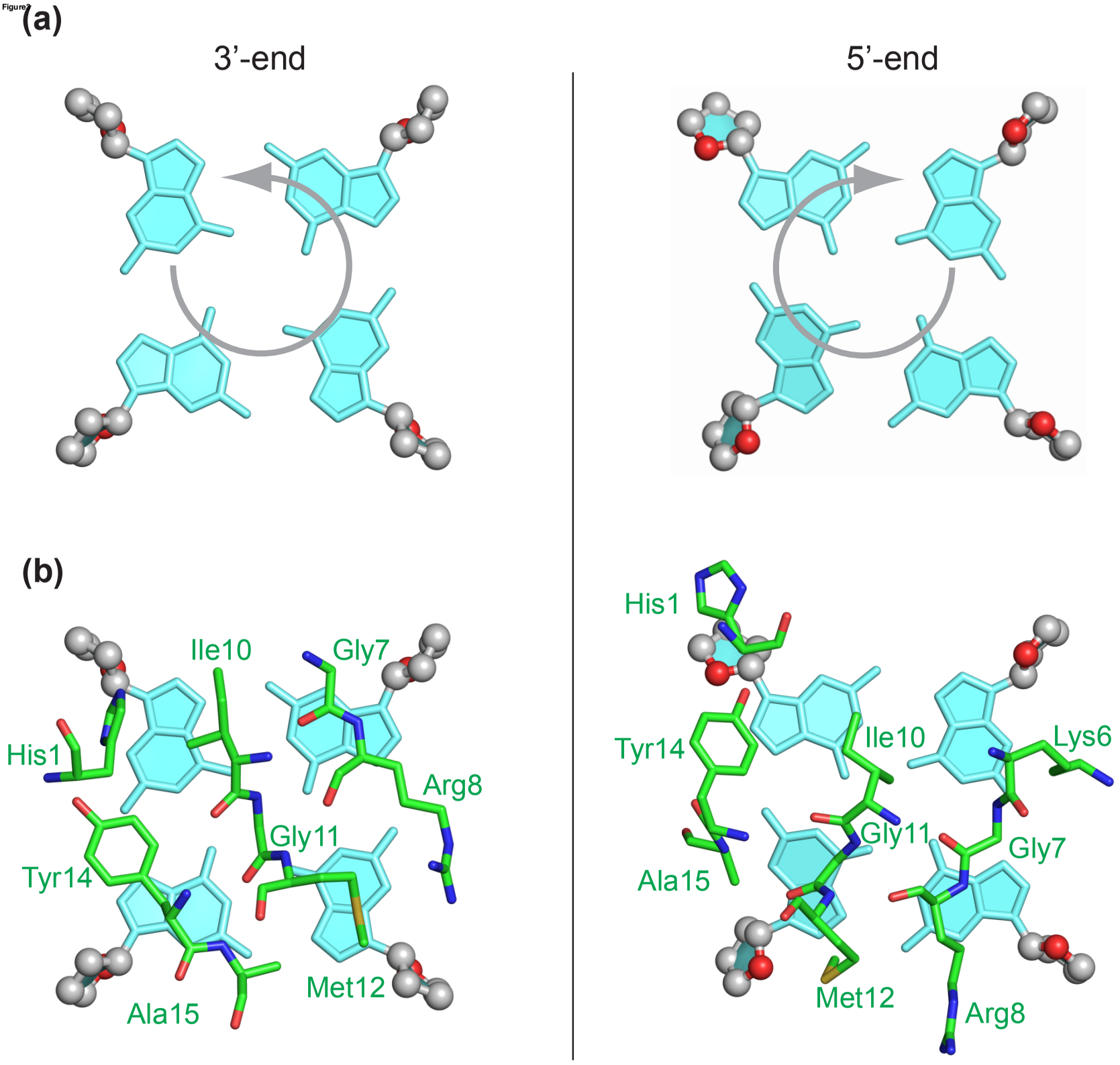
(a)
3’-end
5’-end
(b)
His1
Ile10
Gly7
Arg8
Gly11
Tyr14
Met12
Ala15
His1
Tyr14
Ile10
Lys6
Gly11
Gly7
Ala15
Met12
Arg8